

't Hooft Loops, Electric Flux Sectors and Confinement in $SU(2)$ Yang-Mills Theory

Philippe de Forcrand

Institut für Theoretische Physik, ETH Hönggerberg, CH-8093 Zürich, Switzerland

CERN, Theory Division, CH-1211 Genève 23, Switzerland

Lorenz von Smekal

Institut für Theoretische Physik III, Universität Erlangen-Nürnberg, Staudtstr. 7, D-91058 Erlangen, Germany

(October 29, 2018)

We use 't Hooft loops of maximal size on finite lattices to calculate the free energy in the sectors of $SU(2)$ Yang-Mills theory with fixed electric flux as a function of temperature and (spatial) volume. Our results provide evidence for the mass gap. The confinement of electric fluxes in the low temperature phase and their condensation in the high temperature phase are demonstrated. In a surprisingly large scaling window around criticality, the transition is quantitatively well described by universal exponents and amplitude ratios relating the properties of the two phases.

PACS numbers: 12.38.Gc, 12.38.Aw, 11.15.Ha

CERN-TH/2001-197, FAU-TP3-01/7

Center symmetry is widely believed to play a key role for confinement. In $SU(N)$ Yang-Mills theory at finite temperature, the Polyakov loop is commonly used in lattice studies to illustrate this role. Its correlations are short range at low temperature and acquire a non-zero disconnected part above a critical temperature T_c , signaling deconfinement. The role of the low (high) temperature phase as the center symmetric (broken) one is thereby the opposite from that in the corresponding \mathbb{Z}_N -spin model. This suggests to consider dual variables, whose behavior as a function of temperature is reversed. That point of view was emphasized by 't Hooft with the introduction of the dual to the Wilson loop [1]. Temporal 't Hooft loops in $SU(2)$ show screening for the interaction of a static pair of center monopoles in both phases, for $T < T_c$ and for $T > T_c$ [2,3], just as spatial Wilson loops exhibit an area law in either case. The expectation values of (sufficiently large) spatial 't Hooft loops $\widetilde{W}(C)$, on the other hand, change from a screening behavior below T_c to a confined one [4] with a dual string tension $\tilde{\sigma}$ and an area law in the “electrically” deconfined phase above T_c [3],

$$\langle \widetilde{W}(C) \rangle \sim \exp\{-\tilde{\sigma}(T) LR\}, \quad \text{at } T > T_c, \quad (1)$$

for a rectangular curve C spanning a spatial surface of size $L \times R$ on a $1/T \times L^3$ lattice. Ref. [3] also confirmed numerically a perimeter law for 't Hooft loops at $T = 0$.

The qualitative behavior of the spatial 't Hooft loops is thus the same as that of the Wilson loops in the 3-dimensional \mathbb{Z}_2 gauge theory [5]. Furthermore, as the phase transition is approached (from above), the temperature dependence of the $SU(2)$ dual string tension obeys the same scaling law as that of the interface tension in the 3-dimensional Ising model (below T_c). This similarity is expected, since the 3d \mathbb{Z}_2 gauge theory, its dual the 3-dimensional Ising model, and $SU(2)$ at finite temperature all belong to the same universality class.

To introduce a spatial 't Hooft loop of maximal size

$L \times L$, living in, say, the (x, y) plane of the dual lattice, one multiplies one plaquette in every (z, t) plane of the original lattice by a non-trivial element of the center of $SU(N)$ in such a way that the modified plaquettes form a coclosed set. This creates a \mathbb{Z}_N -interface which is equivalent to enforcing boundary conditions with twist in the (z, t) directions. Combining two and three maximal $L \times L$ 't Hooft loops in orthogonal spatial planes yields the partition functions of $SU(N)$ Yang-Mills theory on finite lattices for all possible combinations of temporal twists. From these, one obtains the free energies in the presence of fixed units of electric flux $\vec{e} \in \mathbb{Z}_N^3$ via a \mathbb{Z}_N Fourier transform as shown by 't Hooft [6]. This leads to the respective electric-flux superselection sectors of the theory in the thermodynamic limit. In the present paper, we verify for $SU(2)$ that the partition functions of electric fluxes $\vec{e} \neq 0$ vanish exponentially with the spatial size L of the system for $T < T_c$ in the magnetic Higgs phase with electric confinement, whereas for $T > T_c$ they become equal to that of the neutral $\vec{e} = 0$ sector. Describing the transition by critical exponents of the 3d-Ising class, we discuss how universal amplitude ratios quantitatively relate the two phases, in particular, the string tension below and the dual (vortex) string tension above T_c .

As expected, the free energy F_q of a static fundamental charge jumps from $+\infty$ to 0 at T_c . One might expect to see this also in measuring the Polyakov loop P directly on the lattice. If $\langle P \rangle \equiv e^{-\frac{1}{T}F_q}$, an infinite free energy amounts to a center symmetric distribution, while a non-zero expectation value $\langle P \rangle$ is obtained for finite F_q . However, the presence of a single charge is incompatible with periodic boundary conditions to measure $\langle P \rangle$. And, like any Wilson loop, $\langle P \rangle$ is subject to UV-divergent perimeter terms, such that $\langle P \rangle = 0$ at all T as the lattice spacing $a \rightarrow 0$. Here, we measure the gauge-invariant, UV-regular free energy of a static fundamental charge in $SU(2)$, and show that it has the expected behaviour, dual to that of a certain type of center vortex. Both provide a well-defined order parameter for the transition [7].

Twisted Boundary Conditions and Electric Fluxes

For the finite-volume partition functions of the pure $SU(N)$ gauge theory, 't Hooft's twisted boundary conditions fix the total number of \mathbb{Z}_N -vortices modulo N that pierce planes of a given orientation. Thus, on the 4-dimensional torus there are N^6 different \mathbb{Z}_N -flux sectors corresponding to the 6 possible orientations for the planes of the twists. These label the inequivalent choices for imposing boundary conditions on the gauge potentials A , which are invariant under the center \mathbb{Z}_N of $SU(N)$. One first chooses $A(x)$ to be periodic with the lengths L_μ of the system in each direction μ up to gauge transformations $\Omega_\mu(x_\perp) \in SU(N)$ which can depend on the components x_\perp transverse to that direction,

$$A(x+L_\mu) = \Omega_\mu(x_\perp) (A(x) - \frac{i}{g} \partial) \Omega_\mu^{-1}(x_\perp). \quad (2)$$

Then, compatibility of two successive translations in a (μ, ν) -plane entails that (no summation of indices)

$$\Omega_\mu(x_\perp + L_\nu) \Omega_\nu(x_\perp) = Z_{\mu\nu} \Omega_\nu(x_\perp + L_\mu) \Omega_\mu(x_\perp) \\ \text{with } Z_{\mu\nu} = e^{2\pi i n_{\mu\nu}/N}, \text{ and } n_{\mu\nu} = -n_{\nu\mu} \in \mathbb{Z}_N. \quad (3)$$

The total number mod. N of center vortices in a (μ, ν) -plane is specified in each sector by the corresponding component of the twist tensor $n_{\mu\nu}$. The spatial ones are given by the conserved, \mathbb{Z}_N -valued and gauge-invariant magnetic flux \vec{m} through the box, $n_{ij} \equiv \epsilon_{ijk} m_k$. The time components $n_{0i} \equiv k_i$ define temporal twist $\vec{k} \in \mathbb{Z}_N^3$.

With the inequivalent choices of boundary conditions, the finite-volume theory decomposes into sectors of fractional Chern-Simons number $(\nu + \vec{k} \cdot \vec{m}/N)$ [8] and states labelled by $|\vec{k}, \vec{m}, \nu\rangle$, where $\nu \in \mathbb{Z}$ is the usual instanton winding number. However, these sectors are not invariant under homotopically non-trivial gauge transformations $\Omega[\vec{k}, \nu]$ which can change \vec{k} and ν ,

$$\Omega[\vec{k}', \nu'] |\vec{k}, \vec{m}, \nu\rangle = |\vec{k} + \vec{k}', \vec{m}, \nu + \nu'\rangle. \quad (4)$$

A Fourier transform of the twist sectors $Z(\vec{k}, \vec{m}, \nu)$ which generalizes the construction of θ -vacua as Bloch waves from ν -vacua in two ways, by replacing $\nu \rightarrow (\nu + \vec{k} \cdot \vec{m}/N)$ for fractional winding numbers and with an additional \mathbb{Z}_N -Fourier transform w.r.t. the temporal twist \vec{k} ,

$$e^{-\frac{1}{T} F(\vec{e}, \vec{m}, \theta)} = \frac{1}{N^3} \sum_{\vec{k}, \nu} e^{-i\omega(\vec{k}, \nu)} Z(\vec{k}, \vec{m}, \nu), \quad (5)$$

yields the free energy $F(\vec{e}, \vec{m}, \theta)$ in an ensemble of states invariant, up to a geometric phase $\omega(\vec{k}, \nu) = 2\pi \vec{e} \cdot \vec{k}/N + \theta(\nu + \vec{k} \cdot \vec{m}/N)$, under the non-trivial $\Omega[\vec{k}, \nu]$ also,

$$\Omega[\vec{k}, \nu] |\vec{e}, \vec{m}, \theta\rangle = \exp\{i\omega(\vec{k}, \nu)\} |\vec{e}, \vec{m}, \theta\rangle. \quad (6)$$

These states are then classified, in addition to their magnetic flux \vec{m} and vacuum angle θ , by their \mathbb{Z}_N -valued *gauge-invariant electric flux* in the \vec{e} -direction [6].

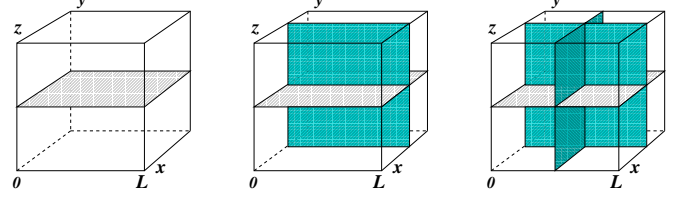


FIG. 1. Cubes with one, two, and three $L \times L$ planes dual to the stacks of flipped plaquettes, sketched for temporal twist $\vec{k} = (0, 0, 1)$, $\vec{k} = (0, 1, 1)$, and $\vec{k} = (1, 1, 1)$ from left to right.

To create $n_{\mu\nu}$ -twist in $SU(2)$, on the lattice, one introduces couplings with reversed signs into the usual Wilson action by replacing $\beta \rightarrow -\beta$ for one plaquette in every (μ, ν) -plane,

$$S(\beta, \vec{k}, \vec{m}) = - \sum_P \beta(P) \frac{1}{2} \text{Tr}(U_P). \quad (7)$$

Herein, the sum extends over all plaquettes P with U_P denoting the path-ordered product of the links around P and we introduced a plaquette-dependent coupling,

$$\beta(P) = \begin{cases} -\beta, & P \in \mathcal{P}(n_{\mu\nu}) \\ \beta, & P \notin \mathcal{P}(n_{\mu\nu}) \end{cases} \quad (8)$$

where $\mathcal{P}(n_{\mu\nu})$ denotes the coclosed stacks of plaquettes dual to the planes of the maximal 't Hooft loops. These stacks of flipped plaquettes force the \mathbb{Z}_2 -interfaces corresponding to twist in the (μ, ν) -directions. Equivalently, they create a 't Hooft loop of maximal size in the orthogonal plane. For the various combinations of temporal twist the coclosed sets $\mathcal{P}(\vec{k})$, when put between two time-slices, can be chosen dual to the spatial planes shown in Fig. 1.

The partition functions of the twist sectors, relative to the untwisted Z_β (such that $Z_\beta(\vec{0}, \vec{0}) = 1$), are then:

$$Z_\beta(\vec{k}, \vec{m}) = Z_\beta^{-1} \int [dU] \exp -S(\beta, \vec{k}, \vec{m}). \quad (9)$$

Similarly, flipping the couplings of plaquettes dual to some surface subtended by a closed curve C yields the expectation value of a finite 't Hooft loop $\widetilde{W}(C)$. An entirely analogous procedure can be used for Wilson loops in the 3-dimensional \mathbb{Z}_2 gauge theory. Through duality, their expectation values can be expressed as ratios of Ising-model partition functions with and without antiferromagnetic bonds at those links of the Ising-model that are dual (in 3 dimensions) to some surface spanned by the \mathbb{Z}_2 -Wilson loop [5]. In both cases the surface is arbitrary except for its boundary. The 't Hooft loop can thus be viewed as a gauge-invariant operator which creates a fluctuating center-vortex surface with pinned boundary.

In this paper, we first calculate $Z_k(\vec{k}) \equiv Z_\beta(\vec{k}, 0)$ for $\vec{m} = 0$ (and $\theta = 0$) on a $1/T \times L^3$ lattice in $SU(2)$ (with k_i in $\{0, 1\}$). The expectation values of maximal-size 't Hooft loops, given by the partition functions of

the twist sectors, are then used to calculate the free energies of electric fluxes as per Eq. (5). For purely temporal twists in particular, the free energies of the electric fluxes through the L^3 box at temperature T , $F_e(\vec{e}; L, T) \equiv F(\vec{e}, \vec{m} = 0, \theta = 0) - F(\vec{e} = 0, \vec{m} = 0, \theta = 0)$, are given by:

$$Z_e(\vec{e}) \equiv e^{-\frac{1}{T}F_e(\vec{e}; L, T)} = \frac{\sum_{\{k_i=0\}}^{N-1} e^{-2\pi i \vec{e} \cdot \vec{k}/N} Z_k(\vec{k})}{\sum_{\{k_i=0\}}^{N-1} Z_k(\vec{k})} \quad (10)$$

with $Z_e(\vec{0}) = Z_k(\vec{0}) = 1$. Because of the invariance under spatial $\pi/2$ rotations, we can write for $SU(2)$: $Z_k(1)$ if $\vec{k} = \{(1, 0, 0), (0, 1, 0), (0, 0, 1)\}$; $Z_k(2)$ if $\vec{k} = \{(1, 1, 0), (1, 0, 1), (0, 1, 1)\}$; and $Z_k(3) = Z_k(1, 1, 1)$, for the partition functions with one, two and three maximal 't Hooft loops in orthogonal spatial planes, respectively. With analogous notations for the $Z_e(\vec{e})$ one thus obtains:

$$Z_e(1) = \frac{1}{\mathcal{N}_e} (1 + Z_k(1) - Z_k(2) - Z_k(3)) , \quad (11)$$

$$Z_e(2) = \frac{1}{\mathcal{N}_e} (1 - Z_k(1) - Z_k(2) + Z_k(3)) , \quad (12)$$

$$Z_e(3) = \frac{1}{\mathcal{N}_e} (1 - 3Z_k(1) + 3Z_k(2) - Z_k(3)) , \quad (13)$$

$$\text{with } \mathcal{N}_e = 1 + 3Z_k(1) + 3Z_k(2) + Z_k(3) .$$

Eqs.(11)-(13) are readily inverted via inverse \mathbb{Z}_2 Fourier transform, which in effect interchanges $Z_e(i) \leftrightarrow Z_k(i)$.

We now establish the connection with Polyakov loops. First, recall that the gauge invariant definition of the latter in the presence of temporal twists is given by [9],

$$P(\vec{x}) = \frac{1}{N} \text{tr} \left(\mathcal{P} e^{ig \int_0^{1/T} A_0(\vec{x}, t) dt} \Omega_t(\vec{x}) \right) . \quad (14)$$

Successively transforming the path-ordered exponential by the various spatial transition functions which accompany the possibly non-trivial $\Omega_t(\vec{x})$ for the transition in the time direction, we derive from (2) and (3) that

$$\begin{aligned} P(\vec{x} + L\vec{e}) &= e^{2\pi i \vec{e} \cdot \vec{k}/N} P(\vec{x}) , \text{ or} \\ P(\vec{x}) P^\dagger(\vec{x} + L\vec{e}) &= e^{-2\pi i \vec{e} \cdot \vec{k}/N} \mathbb{1} . \end{aligned} \quad (15)$$

This is proportional to the unit operator when acting on the states in a sector of definite \vec{k} -twist. Therefore, the electric-flux partition functions of Eq. (10) are in fact the expectation values of Polyakov loop correlators in the ensemble average over all these temporal twists,

$$Z_e(\vec{e}) = e^{-\frac{1}{T}F_e(\vec{e}; L, T)} = \langle P(\vec{x}) P^\dagger(\vec{x} + L\vec{e}) \rangle_{L, T} . \quad (16)$$

This expectation value is taken in the no-flux ensemble, with enlarged partition function $Z = \sum_{\{k_i=0\}}^{N-1} Z_k(\vec{k})$, which is manifestly different, in a finite volume, from the periodic ensemble. Also note that the operator in Eq. (16) has no perimeter, is UV-regular, and we will see that there is no Coulomb term for small volumes either.

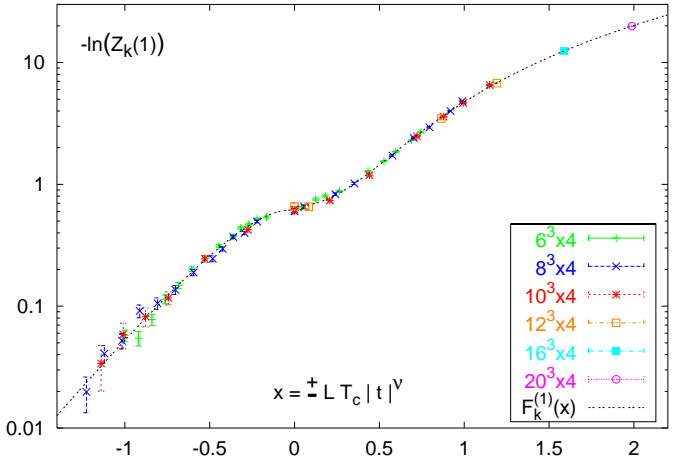


FIG. 2. The free energy of one temporal twist as a function of the finite size scaling variable x (with $x < 0$ for $T < T_c$).

Eq. (10) thus yields a dual relation between Polyakov loops and temporal twists of the general pattern,

$$\langle P(\vec{x}) P^\dagger(\vec{x} + L\vec{e}) \rangle \xrightarrow{L \rightarrow \infty} \begin{cases} 0, & \text{for } Z_k(\vec{k}) \rightarrow 1, T < T_c \\ 1, & \text{for } Z_k(\vec{k}) \rightarrow 0, T > T_c \end{cases}$$

reflecting the different realizations of the electric \mathbb{Z}_N center symmetry in the respective phases.

Finite Size Scaling and Universal Amplitude Ratios

We compute the three partition functions $Z_k(i)$ for $SU(2)$ near T_c by Monte Carlo, using the method of Ref. [3], with 20k–50k measurements per simulation. For pioneering related work at $T = 0$, see Ref. [10]. The $Z_k(i)$ are the analogues of ratios of 3d-Ising model partition functions with different boundary conditions. As for the latter [11], we assume their L, T dependence to be governed by simple finite-size scaling laws,

$$Z_k(i) = f_\pm^{(i)}(x) , \quad i = 1,..3 . \quad (17)$$

The $f_\pm^{(i)}$ are functions of the finite-size scaling variable

$$x = \pm LT_c|t|^\nu \propto L/\xi_\pm(t) , \text{ for } T \gtrless T_c , \quad (18)$$

where $t = T/T_c - 1$ and $\xi_\pm(t) = \xi_\pm^0 |t|^\nu$ are the reduced temperature and the correlation lengths, respectively, and we use the exponent $\nu = 0.63$ from the Ising model.

In our calculations we keep the number of points N_t in the time direction fixed and control the temperature by varying the lattice coupling β around the critical value for the phase transition β_c . The results presented here are obtained with $N_t = 4$ for which $\beta_c = 2.29895(10)$ [12]. We employ couplings β between 2.19 and 2.5 for various lattices ranging from $N_l = 6$ up to $N_l = 20$ points in the spatial directions. Our method to calculate a partition function for one temporal twist amounts to N_l^2 independent Monte Carlo simulations [3]. For a fixed statistical accuracy, which introduces another factor N_l^2 , the cost of the calculation roughly increases as N_l^7 .

For the temperature $T = 1/(N_t a)$, where the lattice spacing $a \equiv a(\beta)$ depends on the coupling, we adopt the leading scaling behavior around criticality of the form,

$$T/T_c = \exp\{b(\beta - \beta_c)\}. \quad (19)$$

The non-perturbative coefficient herein, we use $b = 3.26$, is determined so as to reproduce the published values of $\beta_c(N_t)$ also for $N_t = 6$ and 8 [13].

We can see in Fig. 3 that all our curves intersect at the same point $T = T_c$, which is consistent with the known value of β_c , even for our smallest lattice size. In fact, this intersection point is known to provide a quite accurate determination of the critical coupling β_c already on very small lattices in the Ising model [11].

Away from criticality, corrections to (19) will become important if one is interested in a more precise definition of the physical temperature for $SU(2)$, as in Ref. [13]. Especially at our lowest β values, where such corrections are noticeable, scaling violations become important also. A more refined definition of the reduced temperature t is therefore beyond the scope of our scaling analysis which concerns the dominant behavior near T_c . It has no effect on the qualitative conclusions emphasized here.

That our results for all different lattice sizes nicely collapse on a single curve can be seen for one spatial 't Hooft loop in Fig. 2, with analogous results for $i=2$ and 3. We fit the free energies by an Ansatz for each phase, where the two leading terms obey the expected thermodynamic behavior, while the others represent an ad-hoc modeling of small-size corrections (with $a_{\pm}^{(i)} \sim c_{\pm}^{(i)} < b_{\pm}^{(i)}; d_{\pm}^{(i)} < 1$),

$$F_k^{(i)}(x) = \begin{cases} \exp\left\{b_{-}^{(i)}x + a_{-}^{(i)} - \frac{c_{-}^{(i)}}{(d_{-}^{(i)}-x)^2}\right\}, & x < 0 \\ b_{+}^{(i)}x^2 - a_{+}^{(i)} + \frac{c_{+}^{(i)}}{d_{+}^{(i)}+x^2}, & x > 0 \end{cases} \quad (20)$$

and $-\ln f_{\pm}^{(i)}(x) \equiv F_k^{(i)}(x)$ for $x \gtrless 0$. Plotted over temperature, the data of Fig. 2 and the unique function $F_k^{(1)}(x)$ lead to the family of curves shown in Fig. 3 (top) in which the phase transition is exhibited most clearly. The amplitudes relevant to the large size behavior of the free energy near criticality come out as $b_{-}^{(1)} = 3.87 \pm 0.5$ and $b_{+}^{(1)} = \tilde{\sigma}_0^{(1)} = 5.36 \pm 0.1$, with some additional systematic uncertainty inherent in the form of our Ansatz (20). With analogous data and fits for $Z_k(2)$ and $Z_k(3)$, from Eq. (11), we obtain $Z_e(1)$ as shown in Fig. 3 (bottom). Corrections to scaling do not become appreciable up to $T \sim 2T_c$ indicating a surprisingly large scaling window.

Above T_c , the dual string tension is (with $\tilde{\sigma}_0^{(1)} = b_{+}^{(1)}$),

$$\tilde{\sigma}(T) = \tilde{\sigma}_0^{(1)} T_c^2 |t|^{2\nu} = R/\xi_+^2(t), \quad (21)$$

where the universal ratio $R \simeq 0.104$ [14,15] is known from the 3d-Ising model. There, $R = \xi_-^2 \sigma_I$ relates the correlation length and the interface tension σ_I for $T < T_c$. Here, Eq. (21) determines the screening length for the

Polyakov loops above T_c , $\xi_+(t) = \sqrt{R/\tilde{\sigma}(T)}$. In addition, the universality hypothesis relates the ratio of the correlation lengths for the Polyakov loops in $SU(2)$ to that of their dual analogue, the correlation lengths of the spins in the 3d-Ising model, as measured in Ref. [15],

$$\xi_-^{SU(2)}/\xi_+^{SU(2)} \stackrel{!}{=} \xi_+^{\text{Ising}}/\xi_-^{\text{Ising}} \simeq 1.96. \quad (22)$$

Together with (21) this relates the string tension amplitude below to its dual counter part above T_c , as follows. From the linear part of the electric-flux free energy,

$$\langle P(\vec{x})P^\dagger(\vec{x} + L\vec{e}_i) \rangle \rightarrow e^{-\sigma(T)L/T} = e^{-L/\xi_-(t)}, \quad T < T_c \\ \Rightarrow -\ln(Z_e(1)) \rightarrow -x/(\xi_-^{(0)} T_c), \quad -x = LT_c |t|^\nu, \quad (23)$$

for large L (or $-x$ large). Thus, from Eqs. (21), (22),

$$\frac{\sigma(T)}{T} = \frac{1}{\xi_-(t)} = T_c |t|^\nu \sqrt{\tilde{\sigma}_0^{(1)}/R_+}, \quad R_+ = \frac{\xi_-^2}{\xi_+^2} R \simeq 0.4$$

A value of about $\tilde{\sigma}_0^{(1)} \simeq 5.36$ then implies for the string-tension amplitude $1/(\xi_-^{(0)} T_c) \simeq 3.66$. This value was used in the fit for the slope of the linear part of $-\ln(Z_e(1))$ shown in Fig. 4. Fitting the slope to the data yields the consistent value $1/(\xi_-^{(0)} T_c) = 3.58 \pm 0.5$. This is the linear potential between static charges without Coulomb part.

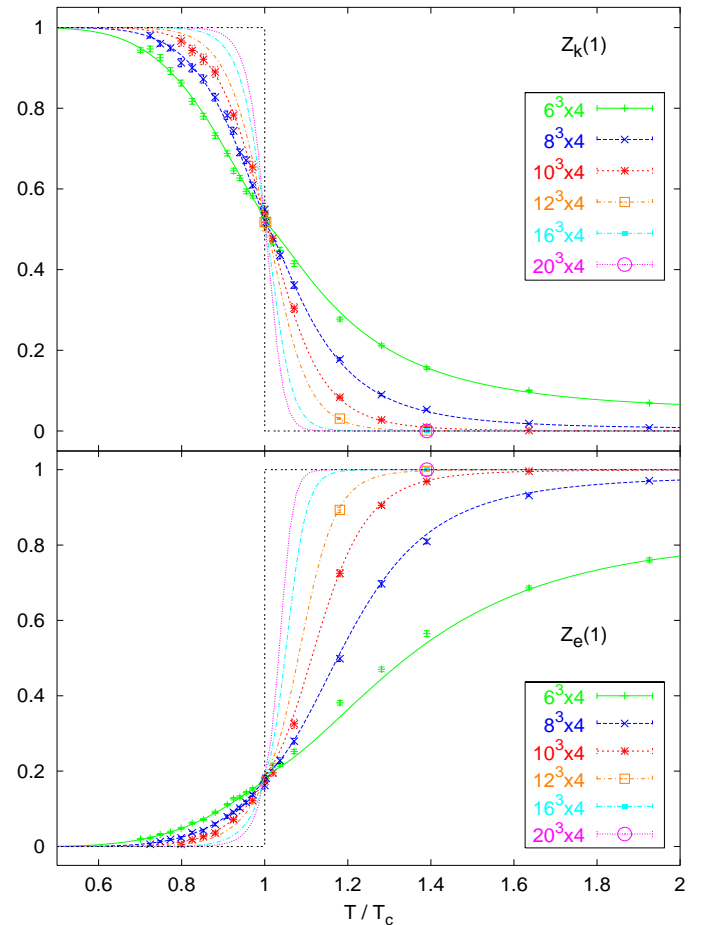


FIG. 3. The partition functions of one temporal twist (top) and one electric flux (bottom) over T for the various lattices.

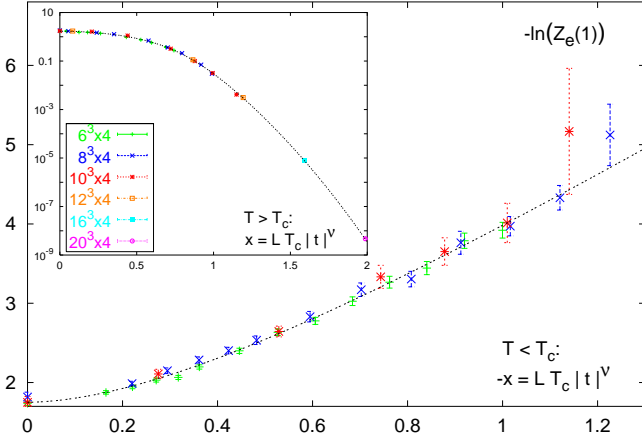


FIG. 4. Free energy of one unit of electric flux from Eq. 11 as a function of x in the confined phase, and above T_c (insert).

The insert of Fig. 4 shows the quality of the finite size scaling from the more accurate data for the free energy of one electric flux in the high temperature phase.

Similar results are obtained from Eqs. (12), (13) also for 2 and 3 orthogonal electric fluxes which we verify to be suppressed more strongly in the confined phase, $Z_e(2)/Z_e(1), Z_e(3)/Z_e(1) \rightarrow 0$ for $L \rightarrow \infty$. Then, inverting Eqs. (11)-(13) one therefore deduces

$$\begin{aligned} -\ln(Z_k(1)) &\rightarrow -\ln(1 - 2Z_e(1)) \sim Z_e(1), \quad T < T_c \\ \Rightarrow 1/(\xi_-^{(0)} T_c) &= b_-^{(1)} = 3.87 \pm 0.5 \end{aligned} \quad (24)$$

for the string tension, which is again consistent with the value $\simeq 3.66$ implied by the universal amplitude ratio. Due to similar relations for $Z_k(2)$ and $Z_k(3)$, we expect $b_-^{(1)} = b_-^{(2)} = b_-^{(3)}$ in our fits (20) for 2 and 3 spatial 't Hooft loops below T_c , which is verified well within our $\mathcal{O}(10\%)$ accuracy on these amplitudes. Above T_c on the other hand, we expect for the dual string tension amplitudes

$$\tilde{\sigma}_0^{(1)} : \tilde{\sigma}_0^{(2)} : \tilde{\sigma}_0^{(3)} \sim 1 : \sqrt{2} : \sqrt{3}, \quad (25)$$

according to the effective area of diagonal loops. In Fig. 5 such a square-root behavior is successfully enforced on the fits (20) of the spatial 't Hooft loops above T_c . We obtain the same ratios, with less accuracy, for the slopes of the electric-flux free energies below T_c , as expected for diagonal fluxes with string formation.

To summarize, we have shown that, below T_c , the free energy of electric fluxes diverges linearly with the length L of the system. Because spatial twists share their qualitative low-temperature behavior with the temporal ones considered here, the free energy of the magnetic fluxes must vanish. This is the magnetic Higgs phase with electric confinement of $SU(2)$ Yang-Mills theory.

At criticality all free energies rapidly approach their finite $L \rightarrow \infty$ limits indicative of massless excitations. We obtain, e.g., $Z_k(1) = 0.54(1)$ for $T = T_c$, which agrees with the corresponding ratio in the 3d-Ising model [15].

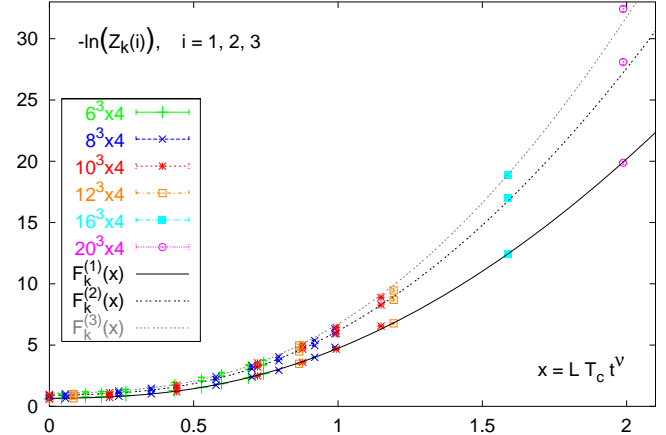


FIG. 5. Free energy of 1, 2 and 3 't Hooft loops at $T > T_c$.

Above T_c , the free energy of electric charges vanishes in the thermodynamic limit. The dual area law prevents magnetic charges from propagating in spatial directions.

The transition is well described by exponents and amplitude ratios of the 3d-Ising class, see also [16].

We are grateful to P. van Baal, M. García Pérez, F. Gliozzi, C. Korthals-Altes, A. Kovner, J. Pawłowski, M. Pepe and H. Reinhardt for discussions. L.v.S. is indebted to the CERN Theory Division for his visiting appointment during which this project was initiated.

-
- [1] G. 't Hooft, Nucl. Phys. **B138** (1978) 1.
 - [2] T. G. Kovács, E. T. Tomboulis, Phys. Rev. Lett. **85** (2000) 704; Ch. Hoelbling, C. Rebbi, V. A. Rubakov, Phys. Rev. **D63** (2001) 034506.
 - [3] Ph. de Forcrand, M. D'Elia, M. Pepe, Phys. Rev. Lett. **86** (2001) 1438.
 - [4] C. Korthals-Altes, A. Kovner, M. Stephanov, Phys. Lett. **B469** (1999) 205.
 - [5] R. Savit, Rev. Mod. Phys. **52** (1980) 453.
 - [6] G. 't Hooft, Nucl. Phys. **B153** (1979) 141; see also, G. 't Hooft in *Confinement, Duality, and Nonperturbative Aspects of QCD*, Plenum Press, New York, 1998.
 - [7] Ph. de Forcrand and L. von Smekal, Nucl. Phys. Proc. Suppl. **106** (2002) 619.
 - [8] P. van Baal, Commun. Math. Phys. **85** (1982) 529.
 - [9] P. van Baal, PhD Thesis, Rijksuniv. Utrecht (1984).
 - [10] A. Hasenfratz, P. Hasenfratz and F. Niedermayer, Nucl. Phys. **B329** (1990) 739.
 - [11] M. Hasenbusch, Physica A **197** (1993) 423; see also Habil. Thesis, Humboldt Univ. Berlin (1999), and refs. therein.
 - [12] J. Engels, S. Mashkevich, T. Scheideler and G. Zinovev, Phys. Lett. **B365** (1996) 219.
 - [13] J. Fingberg, U. Heller and F. Karsch, Nucl. Phys. B **392** (1993) 493.
 - [14] S. Klessinger, G. Münster, Nucl. Phys. **B386** (1992) 701.
 - [15] M. Hasenbusch and K. Pinn, Physica A **192** (1993) 342; *ibid* **203** (1994) 189; *ibid* **245** (1997) 366.
 - [16] M. Pepe and Ph. de Forcrand, Nucl. Phys. Proc. Suppl. **106** (2002) 914.